SUPPORTING INFORMATION

for the

Behavior of silver nanoparticles in wastewater: systematic investigation on the combined effects of surfactants and electrolytes in the model systems

Ivona Capjak[1], Maja Zebić Avdičević[2], Maja Dutour Sikirić[3], Darija Domazet Jurašin[3], Amela Hozić[3], Damir Pajić[4], Slaven Dobrović[2], Walter Goessler[5], Ivana Vinković Vrček[6,1]

[1] Croatian Institute of Transfusion Medicine, Petrova 3, 10 000 Zagreb, Croatia

[2] University of Zagreb, Faculty of Mechanical Engineering and Naval Architecture, Ivana Lučića 5, Zagreb, Croatia

[3] Ruđer Bošković Institute, Bijenička cesta 54, 10 000 Zagreb, Croatia

[4] University of Zagreb, Faculty of Science, Physics Department, Bijenička cesta 32, 10000 Zagreb, Croatia

[5] Institute for Medical Research and Occupational Health, Ksaverska cesta 2, 10 000 Zagreb, Croatia

---

[1] Corresponding author. E-mail address: ivinkovic@imi.hr. Tel.: +385 1 4682540; fax: +385 1 4673303

Superparamagnetic properties of AgNPs

The temperature dependences of magnetization M(T) measured in different applied magnetic fields H and the isothermal field dependences of magnetization M(H) measured at different temperatures T are presented in Figure 2. For all temperatures there is clearly seen linearly decreasing M(H) dependence at higher fields. This slope is approximately the same for all curves, reflecting the temperature independent diamagnetic contribution, and its value of -0.003 $Am^2kg^{-1}T^{-1}$ is in agreement with the diamagnetic susceptibility of silver. Above 50 K M(H) are fully linear, showing dominantly the diamagnetic contribution. However, interesting S-curved features around central part of the M(H) curves appear at 50 K and below. This is a signature of the large magnetic moments superposed onto the mentioned diamagnetic behaviour. Therefore, the measured M(H) dependence is modelled with the Langevin function L(x) with added diamagnetic background, i.e. $M(H)=M_s \cdot L(\mu\mu_0 H/kT)+\chi_d$, where M_s is saturation magnetization, μ magnetic moment, μ_0 absolute magnetic permeability and k Boltzmann constant. Fitting gives the parameters of magnetic moment μ around 11μB (μB is Bohr magneton) and saturation magnetization Ms around 0.008 Am^2kg^{-1} with the mentioned value of diamagnetic background susceptibility χ_d. The obtained μ is actually an effective magnetic moment which differs for the curves measured at different temperatures and is reliably determined within the interval $\mu=(11\pm3)\mu$B, whereas saturation values are within $M_s=(0.008\pm0.002)Am^2kg^{-1}$. Relatively large deviations are caused by possible numerical transfer between the μ and Ms during the fitting procedure, as well as by the fact that there is relatively wide distribution of the nanoparticles over the sizes, but exact modelling is out of the scope of this work.

The temperature dependence of magnetization points to the paramagnetic behaviour of the system which considerably increases the magnetization below temperature of 20K. This change is smoothly continuous, so that it is not the fact of some phase transition. Fitting of the Curie-Weiss model $M(T)=C/(T-\theta)+const$ to the measured data below 40K is very good, giving the Weiss parameter θ between -0.1K and -0.5K that points to the negligible interaction between the particles and the Curie constant C in agreement with magnetic moments of the particles. Also, the pure silver in bulk form could not develop such paramagnetism at low temperatures. Therefore, we conclude that increase of magnetization comes from the superparamagnetic contribution of silver nanoparticles which have magnetic moment much larger than the single electronic one. This large magnetic moment characterizes single nanoparticles and is in agreement with the analysis of M(H) curves where such large magnetic moments were responsible for the S-shaped curves. This paramagnetism has origin in the nanoparticles as a whole, but not the single silver atoms or bulk piece of silver. It is termed as superparamagnetism because of the large magnetic moment sitting on the isolated magnetic units. Coating of the nanoparticles is crucial for their independence, but also it is reasonable to expect the tuning of magnetic moment with chemistry happening between the functionalized surface and silver core.

The magnetization value is very small if compared to ordinary magnetic materials in form of fine particles (for example, four orders of magnitude smaller than in ferrites), showing that magnetic ordering is not established throughout the whole particles, but only in their smaller

part, i.e. surface part, and located around the unsaturated chemical bonds at the boundary. It is expected that magnetic moment of the nanoparticles becomes bigger for smaller particles because of the considerably increased relative amount of surface atoms. Therefore, the superparamagnetic response visible through S-shaped M(H) curves should be more expressed in smaller particles, than in here investigated nanoparticles having 30 nm diameter.

Table S1. Effect of pH and various electrolytes on the Surface Plasmon Resonance (SPR) peak behavior of AgNPs. UV-VIS measurements were performed for 10 mg/L AgNPs suspended in ultrapure water (UW), in medium with pH 3 and 9, in different electrolytes, and in the presence of dodecylammonium chloride (DDACl), sodium dodecyl sulphate (SDS) and Triton X-100 after 1 h, 4 h and 24 h.

Medium	SPR, nm			Absorbance		
	1 h	4 h	24 h	1 h	4 h	24 h
UW	431	430	430	0.81	0.82	0.81
pH 3	433	429	430	0.82	0.54	0.19
pH 9	435	423	433	0.73	0.62	0.63
0.01 M NaCl	428	427	431	0.71	0.63	0.52
0.1 M NaCl	427	428	428	0.18	0.11	0.002
0.01 M Na_2SO_4	433	433	433	0.56	0.31	0.14
0.1 M Na_2SO_4	433	433	433	0.21	0.13	0.006
0.01 M $MgCl_2$	414	415	418	0.26	0.13	0.006
0.1 M $MgCl_2$	468	468	468	0.19	0.12	0.01
0.01 M $MgSO_4$	441	441	441	0.26	0.2	0.01
0.1 M $MgSO_4$	441	441	441	0.27	0.16	0.02
5 mM DDACl	438	438	441	0.75	0.71	0.68
30 mM DDACl	436	436	436	0.77	0.73	0.68
5 mM DDACl + 0.1 M NaCl	436	436	436	0.32	0.2	0.12
30 mM DDACl + 0.1 M NaCl	436	436	436	0.42	0.3	0.19
0.5 mM SDS	433	433	433	0.78	0.77	0.76
5 mM SDS	433	433	433	0.79	0.77	0.75
15 mM SDS	433	433	433	0.79	0.76	0.71
15 mM SDS + 0.1 M NaCl	433	433	433	0.23	0.16	0.13
0.1 mM Triton X-100	423	423	423	0.73	0.71	0.69
1 mM Triton X-100	423	423	423	0.75	0.76	0.72
0.1 mM Triton X-100 + 0.1 M NaCl	423	423	423	0.16	0.1	0.05
1 mM Triton X-100 + 0.1 M NaCl	423	423	423	0.2	0.14	0.03

Table S2. Change of hydrodynamic diameter (d_h) and zeta potential of AgNPs in the presence of dodecylammonium chloride (DDACl), sodium dodecyl sulphate (SDS) and Triton X-100 after 1 h, 4 h and 24 h at 25 °C. The mean volume % of particle populations with different sizes are denoted.

Medium	Popula-tions	1 h		4h		24h	
		d_H (nm)	% mean volume	d_H (nm)	% mean volume	d_H (nm)	% mean volume
Ultrapure water	Peak I	19,54±5,17	82,2	19,40±4,82	80,6	19,39±4,94	84,6
	Peak II	60,70±4,49	17,8	59,87±5,39	19,4	56,36±2,68	15,4
0,1 mM Triton X-100	Peak I	26,65±1,82	100,0	25,70±1,79	100,0	14,41±0,97	78,3
	Peak II	/	/	/	/	54,18±1,52	21,7
1 mM Triton X-101	Peak I	25,09±3,04	76,4	25,70±1,85	75,4	28,14±2,90	76,5
	Peak II	52,56±6,59	28,8	54,71±3,74	24,6	55,89±1,08	23,5
0,05 mM DDACl	Peak I	/	/	16,62±0,91	59,5	/	/
	Peak II	/	/	52,64±4,82	40,5	/	/
30 mM DDACl	Peak I	15,35±0,75	72,6	15,16±1,50	72,7	15,162,29±	70,38
	Peak II	55,41±1,66	27,4	55,18±1,96	27,3	54,50±3,62	29,7
0,5 mM SDS	Peak I	20,73±6,50	79,4	23,70±2,91	79,9	23,87±2,04	82,6
	Peak II	53,52±3,50	20,6	52,56±3,52	20,0	55,21±0,38	17,4
15 mM SDS	Peak I	22,94±1,21	75,0	27,41±2,78	78,1	25,38±2,45	76,5
	Peak II	54,20±5,60	24,9	57,58±2,84	21,9	55,93±2,03	23,5

Table S3. Change of zeta potential of AgNPs in the presence of dodecylammonium chloride (DDACl), sodium dodecyl sulphate (SDS) and Triton X-100 after 1 h, 4 h and 24 h at 25 °C. The mean volume % of particle populations with different sizes are denoted.

Medium	1 h	4h	24h
Ultrapure water	-45,53±0,72	-43,31±3,03	-33,31±3,03
0,5 mM SDS	-38,03±2,13	-29,51±1,90	-45,13±0,97
15 mM SDS	-52,00±1,65	-50,85±1,48	-51,91±2,01
0,1mM TRITON X-100	-25,35±2,07	-25,08±1,69	-25,25±2,28
1 mM TRITON X-100	-24,80±0,58	-24,23±1,13	-21,83±1,26
5 mM DDACl	47,53±1,20	35,08±0,41	18,42±1,54
30 mM DDACl	59,55±1,22	48,99±4,81	43,50±5,98
0,1 M NaCl	-41,90±2,40	-41,40±1,98	-48,92±5,50
1 mM TRITON X-100 + 0,1 M NaCl	-11,89±1,86	-12,70±0,73	-13,27±0,88
15mM SDS + 0,1M NaCl	-41,70±2,32	-34,78±2,70	-35,23±1,67
5 mM DDACl + 0,1 M NaCl	23,48±1,94	25,75±2,40	31,75±1,32
30 mM DDACl + 0,1 M NaCl	50,40±1,85	51,83±5,21	59,924,62±
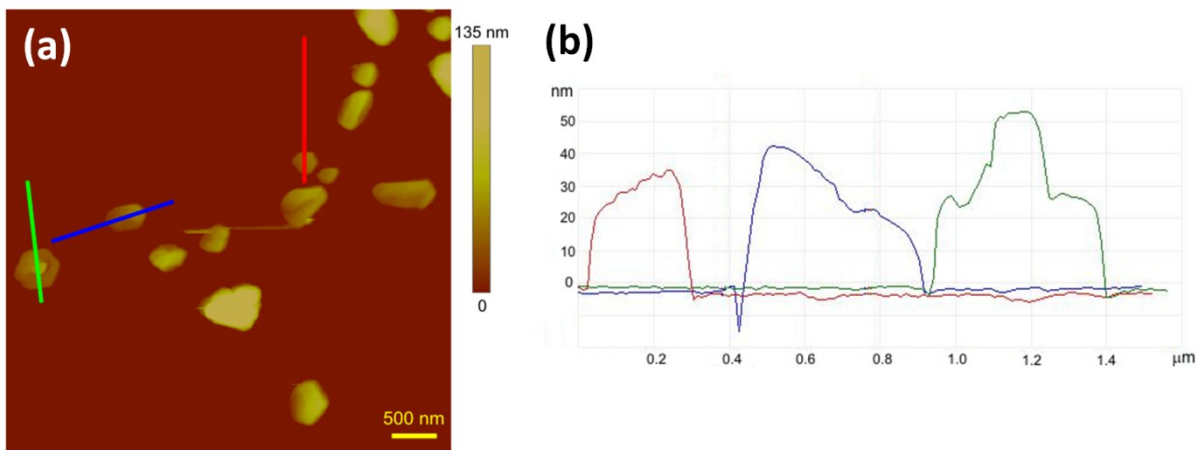
Figure S1. Atomic force microscopy images of AgNPs in ultrapure water: (a) top view of height data, scan size 1 μm x 1 μm, vertical scale 30 nm, (b) section analysis along indicated lines.